Energy dependence of bound-electron–positron pair production at very-high-energy ion-ion transits

A. J. Baltz
Physics Department, Brookhaven National Laboratory, Upton, New York 11973

M. J. Rhoades-Brown
Relativistic Heavy Ion Collider Project, Brookhaven National Laboratory, Upton, New York 11973

J. Weneser
Physics Department, Brookhaven National Laboratory, Upton, New York 11973

(Received 4 June 1991)

The problem of calculating the cross section for bound-electron–positron pair creation in very-high-energy heavy-ion colliders (100 GeV/u or higher, an effective $\gamma \gtrsim 2\times 10^4$) is addressed. The multipole decomposition of the basic time-varying interaction is explicitly written in terms of simple and compact forms that display the energy (γ) dependence directly. Then, specific gauge transforms remove the γ dependence for smaller impact parameters, up to negligible terms of higher order in $1/\gamma$. For larger impact parameters b, the interaction is shown to weaken as $1/b$, where the known perturbative results apply. Only at small impact parameters are strong-coupling calculations necessary, but the gauge choices show that the contributions from these regions are γ independent. Putting these results together leads to a simple form for the cross section, $A\ln\gamma + B$, where A and B are energy independent and A is known from the perturbative calculations. This form and its weak dependence on energy makes extrapolation from lower-energy results reliable and indicates the usefulness of a possible experiment at comparatively low energies ($\gamma \sim 200$).

PACS number(s): 34.90.+q, 34.20.−b

I. INTRODUCTION

The production of bound-electron–positron pairs by the electromagnetic fields of the highly charged ions of relativistic heavy-ion colliders limits the beam lifetime in an important way [1]. Although the problem has been studied with perturbation theory for some time [2,3], recent developments force a reexamination [4]. The high charge states of the ions ($\alpha Z \sim 0.6$ for Au+Au interactions) put into question the earlier perturbation results. In particular, a number of recent papers [5] indicate that standard perturbation approximations, such as the Weizsacker-Williams one, strongly underestimate the electron-capture cross section, at least at moderate impact distances of $\sim \hbar/m_e c$. Furthermore, the very high effective energy (equivalent fixed target Lorentz $\gamma \gtrsim 2\times 10^4$) of the Relativistic Heavy Ion Collider (RHIC) machine now under construction appears to make the nonperturbative problem formidable.

This paper presents a reformulation that removes this latter set of problems and reduces the calculational problem to a much more manageable domain. It further indicates how results at lower energies could be used to safely extrapolate to the regions of the ion colliders by presenting a very general and simple form for the energy dependence of the cross section.

In Sec. II, we examine the basic step of the calculational technology: the multipole expansion. In a departure from past work, an expansion in $1/\gamma$ produces the multipole expansion as compact, explicit, and simple functions of space and time; in Sec. III, comparison with numerical evaluations demonstrates the accuracy of these forms. The consequent availability of these multipole forms permits us to see that the γ dependence appears in just one special term, and that term is *removable* by a gauge transformation. Section IV is devoted to the study of this and other gauge transformations that allow for the removal of the γ dependence, so long as the impact parameter b is well below $\gamma\hbar/m_e c$. Each of the various gauge transformations leads to an effective interaction that is specifically convenient for a particular calculational procedure. Of overriding importance is the clear demonstration that the strength of the interaction falls as $1/b$, thereby becoming weak enough to validate perturbation theory. Section V shows that in this large-b region the perturbational result reduces to the Weizsacker-Williams approximation; contributions to the cross section accumulate up to the natural cutoff at $b \sim \gamma\hbar/m_e c$ to add up to a value of the form $A\ln\gamma + B_{\rm pert}$, where A and $B_{\rm pert}$ are γ independent and known. Adding in the contribution of the small-b region, which as noted, is γ independent, gives us a cross section of the form

$$\sigma = A\ln\gamma + B \ ,$$

where A is known from the perturbation calculation [3] (7.80 ± 0.06 b for fully stripped Au+Au).

This general law for the weak energy dependence of the cross section makes the results of possible lower-energy experiments directly applicable to the very high

energies of the colliders of the future. Experiments at the CERN heavy ion Super Proton Synchrotron (SPS), $\gamma \sim 200$, could be useful, even though the screening of the target prevents precise comparison with the fully stripped ions of the collider. The importance of the cross-section formula comes from the weakness of the energy dependence; a logarithmic increase means that even low energies are near the high energies of the future.

II. CLASSICAL FORM OF THE INTERACTION

The motion of the relativistic heavy ions is assumed to be well described by straight line, classical paths and unperturbed by recoil effects. Since we are interested in the pair production process in which the electron ends in a bound orbit centered on one of the ions, it is useful to fix the coordinate system on that ion. The interaction of the electron field with the moving ion (projectile) is then given by the transformed Coulomb potential

$$V_p(\boldsymbol{\rho},z,t)=\frac{\alpha Z_p(1-v_p\alpha_z)}{\{[(\mathbf{b}-\boldsymbol{\rho})/\gamma]^2+(z-v_pt)^2\}^{1/2}} . \tag{2.1}$$

Here $\mathbf{b}$ is the impact parameter of the projectile ion's path, which is taken along the z axis; Z_p and v_p are the charge and velocity of the projectile; $\gamma=1/(1-v_p^2)^{1/2}$; $\boldsymbol{\rho}$, z, and t coordinates of the electron field relative to the fixed (target) ion; and α_z is the Dirac matrix. To this is added the Coulomb potential of the target ion. The characteristic effects of the electromagnetic interaction produced by the projectile ion V_p are contained in its time dependence and the very severe compression of the spatial dependences—the sharp pulse description found in textbooks.

A more detailed insight into the γ dependence can be obtained from the multipole decomposition of V_p. Such a decomposition is useful if a calculation is to be made in a basis set defined by the Coulomb potential of the target ion; indeed, since our interest is focused on the occupation of the bound orbitals of that potential, such a basis set is central to the analysis. The complex problems of the exact calculation of the scalar multipole,

$$M_l^m(r,t)=\int d\Omega\, Y_l^m\frac{1}{\{[(\mathbf{b}-\boldsymbol{\rho})/\gamma]^2+(z-v_pt)^2\}^{1/2}} , \tag{2.2}$$

have been analyzed and described in several papers [5]. We do not use these methods here. Instead, we derive here simple closed forms for M_l^m that are accurate for large values of γ. Our main purpose in going through these details is the explicit exhibition of the γ dependence, and, thereby, to demonstrate its simple nature. The explicit removal of that dependence is left to Sec. IV.

The derivation consists of an almost straightforward expansion about the near singular point $z=v_pt$, after some careful rearrangement of the integrand. Thus, as a first illustration consider the region $r<v_pt$. Then

$$\begin{aligned} M_l^m&=\int d\Omega\, Y_l^m\frac{1}{|z-v_pt|}+O\left[\frac{\mathbf{b}-\boldsymbol{\rho}}{\gamma}\right]^2 \\ &\simeq\int d\Omega\, Y_l^m\frac{1}{v_pt-r\cos\theta} \\ &=\delta_{m,0}\frac{2\sqrt{\pi}\sqrt{2l+1}}{r}Q_l\left[\frac{v_pt}{r}\right] , \end{aligned} \tag{2.3}$$

where Q_l is the familiar Legendre function of the second kind; it will be recalled that as $r\to v_pt$,

$$Q_l\to\tfrac{1}{2}P_l(1)\ln\frac{2}{v_pt-r}\simeq\tfrac{1}{2}\ln\frac{4}{(v_pt)^2-r^2} .$$

There is need for care at $r\sim v_pt$, which it will indeed receive below. It is important to note that this expansion requires that $b/(r-v_pt)\ll\gamma$; assuming that the nature of the physical problem confines r and v_pt to moderate multiples of $\hbar/m_ec$, the requirement of b becomes $b\ll\gamma\hbar/m_ec$. This limitation on b, however, is an easy burden to carry since we will see later on that at moderate b the Weizsacker-Williams approximation becomes valid and can be merged onto the nonperturbative calculation appropriate for smaller impact parameters.

To carry out the expansion systematically, we write

$$\begin{aligned} M_l^m=&\int d\Omega\frac{1}{\{[(\mathbf{b}-\boldsymbol{\rho})/\gamma]^2+(r\cos\theta-v_pt)^2\}^{1/2}}Y_l^m(\theta_t,\phi) \\ &+\int d\Omega\frac{1}{\{[(\mathbf{b}-\boldsymbol{\rho})/\gamma]^2+(r\cos\theta-v_pt)^2\}^{1/2}}[Y_l^m(\theta,\phi)-Y_l^m(\theta_t,\phi)] , \end{aligned} \tag{2.4}$$

where θ_t is defined by

$$|v_pt|<r,\quad \cos\theta_t=\frac{v_pt}{r} ,\quad \sin\theta_t=[1-(v_pt/r)^2]^{1/2} ;$$

$$|v_pt|>r,\quad \cos\theta_t=1,\quad \sin\theta_t=0 .$$

Since the integrand of the second term remains finite when the $[(\mathbf{b}-\boldsymbol{\rho})/\gamma]^2$ term of the denominator is dropped, it is easy to see that this second term of (2.4) is given to order $\ln\gamma/\gamma^2$ by

$$\int d\Omega \frac{1}{|r\cos\theta - v_p t|}[Y_l^m(\theta,\phi) - Y_l^m(\theta_t,\phi)] = \delta_{m,0}\frac{\sqrt{\pi}\sqrt{2l+1}}{r}\left[\int_{t/r}^{1} dx \frac{P_l(x)-P_l(t/r)}{x-t/r} + \int_{-1}^{t/r} dx \frac{P_l(x)-P_l(t/r)}{t/r-x}\right]$$

$$= \delta_{m,0}\frac{\sqrt{\pi}\sqrt{2l+1}}{r}\left[-2P_l\left[\frac{t}{r}\right]\sum_{n=1}^{l}\frac{1}{n}\right] \quad \text{if } |t|<r \tag{2.5a}$$

and

$$\delta_{m,0}\frac{\sqrt{\pi}\sqrt{2l+1}}{r}\left[2Q_l\left[\frac{t}{r}\right] - \ln\frac{t+r}{t-r}\right] \quad \text{if } |t|>r\ . \tag{2.5b}$$

We have also replaced v^p by 1 since they differ only by $O(1/\gamma^2)$. Both forms are finite and easily computable by standard methods. The first term in Eq. (2.4) is amenable to elementary treatment if it is noted that to order $\ln\gamma/\gamma^2$ the $(\mathbf{b}-\boldsymbol{\rho})^2/\gamma^2$ in the denominator can be replaced by its value at $\theta=\theta_t$, v_p by 1:

$$\int d\Omega \frac{1}{\{[(\mathbf{b}-\boldsymbol{\rho})/\gamma]^2 + (r\cos\theta - t)^2\}^{1/2}} Y_l^m(\theta_t,\phi)$$

$$= Y_l^m(\theta_t,0)\int d\Omega \frac{e^{im\phi}}{\{(b^2/\gamma^2)[1-2(r/b)\sin\theta_t\cos\phi + (r^2/b^2)\sin^2\theta_t] + (r\cos\theta - t)^2\}^{1/2}}$$

$$= \frac{Y_l^m(\theta_t,0)}{r}\int d\phi\, e^{im\phi}\ln\left[\frac{\{[(v_p t/r)-1]^2 + [(b^2/r^2)/\gamma^2](1-(2r/b)\sin\theta_t\cos\phi + (r^2/b^2)\sin^2\theta_t)\}^{1/2} - (1-t/r)}{\{[(v_p t/r)+1]^2 + [(b^2/r^2)/\gamma^2](1-(2r/b)\sin\theta_t\cos\phi + (r^2/b^2)\sin^2\theta_t)\}^{1/2} - (1+t/r)}\right]. \tag{2.6}$$

Except in the narrow region of width of $O(b/\gamma)$ around $v_p t/r \sim 1$, the logarithm can be expanded, so that we have

$$\frac{Y_l^m(\theta_t,0)}{r}\int d\phi\, e^{im\phi}\ln\left[\frac{t+r}{t-r}\right] = \delta_{m,0}\frac{\sqrt{\pi}\sqrt{2l+1}}{r}\ln\left[\frac{t+r}{t-r}\right] \quad \text{if } r<|t|\ ,$$

and if $r>|t|$,

$$\frac{Y_l^m(\theta_t,0)}{r}\int d\phi e^{im\phi}\left[\ln 4\gamma^2 + \ln(r^2-t^2) - \ln b^2\left[1 - \frac{2r}{b}\sin\theta_t\cos\phi + \frac{r^2}{b^2}\sin^2\theta_t\right]\right].$$

Integrating over ϕ we obtain

$$\delta_{m,0}2\pi\frac{Y_l^0(\theta_t,0)}{r}\left\{\ln 4\gamma^2 + \left[1-\theta\left[\frac{r^2-t^2}{b^2}-1\right]\right]\ln\frac{r^2-t^2}{b^2}\right\} + (1-\delta_{m,0})2\pi\frac{Y_l^m(\theta_t,0)}{r}\frac{1}{|m|}$$

$$\times\left[\left[\frac{r^2-t^2}{b^2}\right]^{|m|/2}\theta\left[\frac{b^2}{r^2-t^2}-1\right] + \left[\frac{b^2}{r^2-t^2}\right]^{|m|/2}\theta\left[\frac{r^2-t^2}{b^2}-1\right]\right], \quad \text{if } r>|t|\ ; \tag{2.7}$$

$\theta(x)$ is the familiar step function, 0 if $x<0$ and 1 if $x>0$. Should the narrow region at $r\sim t$ be important in some calculation, instead of approximating the integral of (2.6) in the manner of (2.7), the original form of the integral is to be used with $\theta_t \to 0$ to provide a bridge across the gap:

$$\delta_{m,0}\frac{\sqrt{\pi}\sqrt{2l+1}}{r}\ln\frac{[(t/r-1)^2 + (b^2/r^2)/\gamma^2]^{1/2} + (1-t/r)}{[(t/r+1)^2 + (b^2/r^2)/\gamma^2]^{1/2} - (1+t/r)}\ ; \tag{2.8}$$

in the narrow region around $r\sim t$ the use of this function is reliable to order $1/\gamma$.

In summary, the asymptotic form of the multipole decomposition of $V_p(\boldsymbol{\rho},z,t)$ is given by

$$V_p(\rho,z,t)=\alpha Z_p(1-\alpha_z)\sum_{l,m>0}[Y_l^m(\theta,\phi)+Y_l^{m*}(\theta,\phi)]\frac{Y_l^m(\theta_t,0)}{r}\times\begin{cases}0 & \text{if } r<|t| \\ \frac{2\pi}{m}\left[\frac{r^2-t^2}{b^2}\right]^{m/2} & \text{if } |t|<r<[b^2+t^2]^{1/2} \\ \frac{2\pi}{m}\left[\frac{b^2}{r^2-t^2}\right]^{m/2} & \text{if } r>(b^2+t^2)^{1/2}\end{cases}$$

$$+\alpha Z_p(1-\alpha_z)\sum_l Y_l^0(\theta)\begin{cases}\frac{2\sqrt{\pi}\sqrt{2l+1}}{r}Q_l(t/r) & \text{if } r<|t| \\ \frac{\sqrt{\pi}\sqrt{2l+1}}{r}P_l\left[\frac{t}{r}\right]\left[2\ln 2\gamma+\ln\frac{r^2-t^2}{b^2}-2\sum_{n=1}^{l}\frac{1}{n}\right] & \text{if } |t|<r<(b^2+t^2)^{1/2} \\ \frac{\sqrt{\pi}\sqrt{2l+1}}{r}P_l\left[\frac{t}{r}\right]\left[(2\ln 2\gamma)-2\sum_{n=1}^{l}\frac{1}{n}\right] & \text{if } r>(b^2+t^2)^{1/2}\end{cases} \tag{2.9}$$

As noted, at $r\sim|t|$ the discontinuity is bridged by the logarithm (2.8), so that with inclusion of the finite values of (2.5a) or (2.5b) the $m=0$ multipoles are better described at this delicate point by

$$\alpha Z_p(1-\alpha_z)Y_l^0(\theta)\frac{\sqrt{\pi}\sqrt{2l+1}}{r}\left[\ln\frac{[(t/r-1)^2+(b^2/r^2)/\gamma^2]^{1/2}+(1-t/r)}{[(t/r+1)^2+(b^2/r^2)/\gamma^2]^{1/2}-(1+t/r)}-2\sum_{n=1}^{l}\frac{1}{n}\right]. \tag{2.10}$$

Expansion of the logarithm of Eq. (2.10) in b^2/γ^2 for $r\gtrless|t|$ demonstrates the connection with the two forms written above. However, note that the singularities at $r\sim|t|$ contained in Eq. (2.9) are integrable, and the result of integration across the $r\sim|t|$ region with either form is the same to order $\ln\gamma/\gamma$. Therefore, unless the $m=0$ multipole terms are to be integrated together with functions that vary sharply in the $r\sim|v_pt|$ region, the need for the bridge function disappears. Such a sharp dependence would be possible for matrix elements involving high-momentum wave functions whose oscillation length $1/p$ is of order b/γ. As we shall see later the coupled-channels approach is to be used only for small b, say $\leq 5\hbar/m_ec$; then, for $\gamma\geq 200$, the domain $p\lesssim 40m_ec$ is untroubled.

A feeling for the range of energies that are expected to be of importance can be gleaned from perturbation theory. As will be seen in Sec. V, the perturbative cross section is largely determined by the related photon cross section weighted by an additional factor of inverse photon energy. As can be seen by weighting the calculation of Johnson, Buss, and Carroll [6], the K-captured electron is accompanied by moderate-energy positrons whose spectrum peaks at approximately $1.5m_ec^2$ total energy, and falls very roughly as the square of the energy. We are then dealing with a calculation whose energy domain is confined, as is the spatial domain. It is this picture that we bring along to understand the usefulness of approximations in the full, nonperturbative calculations.

Although in the present work we do not actually evaluate time-dependent matrix elements for use in coupled-channels calculations, we cannot help but notice that such an endeavor will be facilitated by the form of the above interaction. In Eq. (2.9) all terms can be expressed in terms of polynomials and/or convergent series in (t/r) for $t<r$, and in (r/t) for $r<t$. Thus the matrix element to be integrated over r can have its interaction expressed as a series of negative and positive powers of r. In each of the terms of the series in r, t is effectively a coefficient: r and t have become separable term by term.

In addition to providing a simple means of calculating matrix elements, the asymptotic forms obtained above allow us to straightforwardly look at the γ dependence of any set of matrix elements or amplitudes. As we can see directly, the γ dependence of the multipole operators appears only in the $m=0$ terms and only in the one form:

$$(2\ln 2\gamma)\alpha Z_p(1-\alpha_z)\sum_l Y_l^0(\theta)\frac{\sqrt{\pi}\sqrt{2l+1}}{r}P_l\left[\frac{t}{r}\right]$$

$$=(2\ln 2\gamma)\alpha Z_p(1-\alpha_z)\delta(z-t),\quad r>|t|\ ; \tag{2.11}$$

the condition $r\geq|t|$ is automatically contained in the $\delta(z-t)$. But, as we shall see in Sec. IV, this set of terms is entirely removable by a gauge transformation. Once having removed this explicit dependence on γ, we are left only with the implicit dependence inherent in the limitation already noted that the above forms are valid only for the region $b\ll\gamma\hbar/m_ec$. However, as we shall fully discuss later, when b is not small, perturbation theory is valid. This, then, immediately implies a very general result for the total cross section for pair creation with the electron captured into a bound state.

III. COMPARISON WITH EXACT SOLUTIONS

In this section comparisons are made between the analytic forms obtained above as large-γ limits and the exact multipole components. Two methods are employed: (1) an analytic expansion of the interaction in spherical harmonics followed by numerical evaluation of the resultant functions, and (2) direct numerical integration of the angularly weighted interaction. There are complementary advantages to each.

The expansion in spherical harmonics begins with the familiar Fourier form:

$$V_p=\frac{1}{\{[(\boldsymbol{\rho}-\mathbf{b})/\gamma]^2+(z-v_pt)^2\}^{1/2}}$$
$$=\frac{1}{2\pi^2}\int d^2q_\perp dq_z\frac{e^{i\mathbf{q}_\perp\cdot(\boldsymbol{\rho}-\mathbf{b})+iq_z(z-v_pt)}}{q_\perp^2+q_z^2/\gamma^2}$$
$$=\frac{1}{2\pi^2}\int d^3q\frac{e^{i\mathbf{q}\cdot\mathbf{r}}e^{-i(\mathbf{b}+v_pt\hat{\mathbf{z}})\cdot\mathbf{q}}}{q_\perp^2-v_p^2q_z^2}\ . \tag{3.1}$$

Expansion of each of the plane waves in the usual spherical harmonics followed by the azimuthal integration over ϕ_q results in

$$V_p=16\pi\sum_{l,l',m}i^{l-l'}Y_l^m(\theta,\phi)Y_{l'}^m(\theta_u,0)$$
$$\times\left[\int_0^\infty dq\,j_l(rq)j_{l'}(uq)\right]$$
$$\times\left[\int d(\cos\theta_q)\frac{1}{1-v_p^2\cos^2\theta_q}\right.$$
$$\left.\times Y_l^{m*}(\theta_q,0)Y_{l'}^m(\theta_q,0)\right]\ . \tag{3.2}$$

Here $\mathbf{u}$ is the vector $(\mathbf{b}+v_pt\hat{\mathbf{z}})$, u its length $[b^2+(v_pt)^2]^{1/2}$, and θ_u its polar angle; azimuthal angles are measured from the $\mathbf{b}$ axis. The integrals are well known:

$$\int_0^\infty dq\,j_l(rq)j_{l'}(uq)$$
$$=\frac{\pi}{4}\frac{u^{l'}}{r^{l'+1}}\frac{\Gamma((l+l'+1)/2)}{\Gamma((l-l')/2+1)\Gamma(l'+\frac{3}{2})}$$
$$\times F\left[\frac{l+l'+1}{2},\frac{l'-l}{2},l'+\tfrac{3}{2},u^2/r^2\right]\quad\text{if } r>u \tag{3.3a}$$

and the interchange $r\leftrightarrow u$, $l\leftrightarrow l'$ if $r<u$. For the very special case of $r=u$,

$$\int_0^\infty dq\,j_l(rq)j_{l'}(rq)=\frac{\pi}{4}\frac{1}{r}\frac{\Gamma((l+l'+1)/2)}{\Gamma((l'-l)/2+1)\Gamma((l+l')/2+1)\Gamma((l-l')/2+1)}\ ; \tag{3.3b}$$

as notation, we call this set of integrals $\mathcal{R}(l,l';r,u)$. The angular integral is

$$\int d(\cos\theta_q)\frac{1}{1-v_p^2\cos^2\theta_q}Y_l^{m*}(\theta_q,0)Y_{l'}^m(\theta_q,0)$$
$$=\frac{1}{4\pi}(-1)^m\sqrt{(2l+1)(2l'+1)}\sum_L C_{-mm0}^{ll'L}C_{000}^{ll'L}\int d(\cos\theta_q)\frac{P_L(\cos\theta_q)}{1-v_p^2\cos^2\theta_q}$$
$$=\frac{1}{4\pi}(-1)^m\sqrt{(2l+1)(2l'+1)}\sum_L C_{-mm0}^{ll'L}C_{000}^{ll'L}\frac{2}{v_p}Q_L\left[\frac{1}{v_p}\right]=\mathcal{A}(m;l,l';1/v_p)\ . \tag{3.4}$$

The multipole decomposition is then given as the series

$$V_p=\sum_{l,m}Y_l^m(\theta,\phi)\sum_{l'}Y_{l'}^m(\theta_u,0)\mathcal{R}(l,l';r,u)$$
$$\times\mathcal{A}(m;l,l';1/v_p)\ ,$$
$$u=[b^2+(v_pt)^2]^{1/2},\quad\cos\theta_u=\frac{v_pt}{u},\quad\sin\theta_u=\frac{b}{u}\ . \tag{3.5}$$

There is a set of special cases that is particularly simple and informative: For $r>u$ the sum over l' in (3.5) is cut off by the spherical Bessel function integral (3.3a) (the occurrence of a negative-integer value of the argument of the gamma function ensures that $l'\le l$); furthermore, for $l'\lesssim l$ the hypergeometric function is just a polynomial. Thus the exact result for the Y_1^1 component of V_p is

$$Y_1^1(\theta,\phi)\sqrt{3\pi/2}\frac{b}{r^2}\left\{\frac{2}{v_p}\left[-\tfrac{1}{3}Q_0\left[\frac{1}{v_p}\right]+\tfrac{1}{3}Q_2\left[\frac{1}{v_p}\right]\right]\right\}$$
$$=Y_1^1(\theta,\phi)\sqrt{3\pi/2}\frac{b}{r^2}\left[\frac{1}{v_p}\left[\frac{1}{v_p^2}-1\right]Q_0\left[\frac{1}{v_p}\right]\right.$$
$$\left.-\frac{1}{v_p}\right]\quad\text{if } r>u\ , \tag{3.6}$$

$$Q_0=\tfrac{1}{2}\ln\frac{1+v_p}{1-v_p}\ .$$

As $\gamma\to\infty$, $v_p\to1$, the term in square brackets on the right-hand side approaches -1, in agreement with the

corresponding expression of Eq. (2.9). Similarly, the Y_1^0 component of V_p is

$$Y_1^0(\theta,\phi)\sqrt{3\pi}\frac{t}{r}\left[2\frac{1}{v_p^2}Q_0\left[\frac{1}{v_p}\right]-2\right] \quad \text{if } r>u \ ; \tag{3.7}$$

as $\gamma\to\infty$ the term in square brackets approaches $2\ln 2\gamma-2$, in agreement with Eq. (2.9). In both these illustrations it is clear that the difference between exact and asymptotic values is $O(\ln\gamma/\gamma^2)$.

In order to compare with forms for the multipole expansion that appear in the literature, it is noted here that the term

$$Z^{l,m}(\xi,\psi)=\int_0^{\pi}d\theta_S\frac{\sin\theta_S}{1-v_p^2\cos^2\theta_S}e^{-i\xi\sin\psi\cos\theta_S} \times J_m(\xi\cos\psi\sin\theta_S)Y_l^{m\,*}(\theta_S,0) \ ,$$

which is central to the coupled-channel calculations carried out in Ref. [5], may be easily rewritten as the series (3.5) using the identity [7]

$$J_{\nu-1/2}(z\sin\alpha\sin\beta)e^{iz\cos\alpha\cos\beta} =2^{2\nu-1/2}(\pi z)^{-1/2}[\Gamma(\nu)]^2(\sin\alpha\sin\beta)^{\nu-1/2} \times\sum_{n=0}^{\infty}\frac{i^n n!(\nu+n)}{\Gamma(2\nu+n)}J_{\nu+n}(z)C_n^{\nu}(\cos\alpha)C_n^{\nu}(\cos\beta) \ ,$$

where C_n^{ν} are Gegenbauer polynomials. The Gegenbauer polynomials are readily expressed as Legendre polynomials, resulting in Eq. (3.2).

In evaluating the series over l' of Eq. (3.5) we find an oscillatory behavior, especially for $m=0$ terms. These convergence problems can be readily overcome with the aid of Padé approximants [8]. By construction, the kth partial sum is given by the sum of $k+1$ terms of the power series

$$S_k^{l,m}=\sum_{l'=0}^{k}Y_{l'}^m(\theta_u,0)\mathcal{R}(l,l',r,u)\mathcal{A}(m,l,l',1/v_p)x^{l'} \tag{3.8}$$

evaluated at $x=1$. A Padé approximant to the polynomial $S_k^{l,m}(x)$ of order k is a rational function (ratio of polynomials)

$$[L/M]=\frac{P_L(x)}{Q_M(x)} \quad (L+M=k) \ ; \tag{3.9}$$

the coefficients of the Padé polynomials, $P_L(x)$ and $Q_L(x)$, are chosen such that the first k terms of its Taylor series coincide with $S_k^{l,m}(x)$. We use the Wynn algorithm [9] to generate directly the approximants $[L/L]$ and $[L+1/L]$ for $x=1$. Numerical studies show that this sequence of Padé approximants to $S_k^{l,m}(x)$ accelerate the convergence of the original series when it converges, and converge rapidly under circumstances (typically for $m=0$) when the original series is seen to diverge. Extensive numerical studies for combinations of r, t, v_p, b, l, and m values show clearly the reliability and speed of this approach. In general, the largest number of terms for $S_k^{l,m}(x)$ required to achieve convergence occurred near the singular point $r=v_pt$. As examples of the results, for ($l=1$, $m=0$) at $b=1$, $t=20$ and $\gamma=10$, we obtained convergence to better than one part in 10^5 for values of r between 0 and 20. Typically, this measure of convergence is achieved for the [8/8] diagonal element of the Padé table. However, for $b=1$, $t=1$ ($l=1$, $m=0$, $\gamma=10$ as before) convergence of only one part in 10^4 is achieved at the singular point $r=v_pt=1$ for the [9/9] Padé element. Comparison of these Padé accelerated results for a whole range of r, b, t, l, and m values with the numerical method described below shows very close agreement.

Direct numerical integration over the angular coordinates θ and ϕ, for each value of the variables (r,t), provides a standard of known accuracy to which the asymptotic formulation Eqs. (2.9) and (2.10) as well as the alternate exact expansion Eqs. (3.1)–(3.5) can be compared. The basic numerical method used involves a uniform grid in $\Delta\phi$ and $\Delta(\cos\theta)$ (or $\Delta\theta$) and the summation of contributions is evaluated at the center of each interval in the two dimensions. Three variations of this method were employed as appropriate. The first, most straightforward option, was to simply sum elements evaluated on a uniform grid in $\Delta\phi$ and $\Delta(\cos\theta)$. A second, slight variation of this method was employed in which it was assumed that only the $\cos\theta$ terms in the denominator vary over the small interval $\Delta(\cos\theta)$ and thus each element may be analytically integrated over the interval $\Delta(\cos\theta)$. The third method is similar to the second except that the interval chosen for this piecewise analytic integration is uniform in $\Delta\theta$ rather than in $\Delta(\cos\theta)$. With these three methods available, the one most appropriate to the particular r, t, and γ region could be chosen in order to obtain results of sufficient accuracy.

A number of comparisons were made between results of numerical evaluation of the integrals M_1^0, M_1^1, and M_2^1 and results of evaluation using the exact expansion Eqs. (3.1)–(3.5) described above. Agreement between the two exact methods was in every case excellent. The hardest case for both methods occurs in the region $r\approx v_pt$, and our agreement (e.g., M_1^0 at $\gamma=10$, $t=1$, $b=5$) of about one part in 1500 is what we would have roughly estimated in each method independently, based on change of results with mesh size on the one hand and based on the convergence of the Padé approximants on the other. Agreement was no worse than this anywhere else we tested, and agreement between the two exact methods was typically several orders of magnitude better. In comparison between the exact method and the asymptotic expansion which follow, the exact expressions were evaluated by the direct numerical integration.

To compare the asymptotic expressions with exact evaluation of the multiple components, the dipole components $M_1^0(r,t)$ and $M_1^1(r,t)$ have been computed at γ of 10, 200, and 20 000 corresponding to relevant heavy-ion-beam energies at the Brookhaven Alternating Gradient Synchrotron, the CERN SPS, and the RHIC collider now under construction. In the case of RHIC, a 100-GeV/A on 100-GeV/A collider, the γ of 20 000 corresponds to the equivalent energy/A of one ion seen in the rest frame of the other.

We display the radial dependence of the multipole ele-

ments for the combinations of time $t=1$ and 10 and impact parameter $b=1$ and 10. Our unit of length is $\hbar/m_e c$ (386 fm); time is in units of $\hbar/m_e c^2$. The two components $M_1^0(r,t)$ and $M_1^1(r,t)$ are considered in turn.

In Figs. 1–8 we follow a convention that the lines correspond to exact calculations and the discrete symbols correspond to calculations done with the asymptotic form: For $\gamma=10$, the solid line corresponds to the exact form and the circles are the asymptotic form; for $\gamma=200$, the long-dash-dotted line is exact and the triangles the asymptotic form; for $\gamma=20\,000$, the short-dashed line is exact and the squares the asymptotic form.

Figure 1 shows calculations of $M_1^0(r,t=1)$ for an impact parameter b of 1. For $\gamma=20\,000$ and 200 agreement between the exact calculation and the asymptotic form is excellent. For example, for the points $r=0.9,1.0,1.1$, $\gamma=200$, the asymptotic form agrees with the exact to 0.1% or better. For $\gamma=10$ some discrepancy is evident, particularly around $r=t=1$, as expected. In fact, the asymptotic form is 12% low at $r=0.9$, 10% high at $r=1.1$, and 7% high at the bridge point $r=1$. The bridge formula Eq. (2.10) was used only for the one point $r=t=1$, and in subsequent calculations we also make use of the bridge formula only if r is exactly equal to t. Note that for $r<|t|$ the asymptotic formula is independent of γ and the points lie on top of each other.

If b and t are increased to 10, then the discrepancies become larger for $\gamma=10$, especially around $r=t=10$ as we would expect for a formula ignoring terms in $(b/\gamma)^2$ (Fig. 2). And in the final $m=0$ example, in Fig. 3 $b=10$ and $t=1$; $M_1^0(r,t=1)$ is concentrated at small values of t. These curves are similar to those of Fig. 1. However, there is a greater discrepancy in Fig. 3 between the asymptotic form and exact calculations for $\gamma=10$ as would be expected for the larger b.

Calculations for M_1^1 analogous to those of M_1^0 seen in Figs. 1–3 are presented in Fig. 4–6. The general pattern of the asymptotic form for M_1^1 is that it is γ independent (the circles, triangles, and squares are, thus, on top of each other), is zero for $r<t$, increases in magnitude for $t<r<(b^2+t^2)^{1/2}$, and decreases in magnitude for $(b^2+t^2)^{1/2}<r$. For all values of t and b, there is generally excellent agreement between the asymptotic formula and the exact calculation for $\gamma=200$ (long-dash-dotted line) and $\gamma=20\,000$ (short-dashed line) as is evident in Figs. 4–6. These figures also show a systematic discrepancy between the exact calculation for $\gamma=10$ and the asymptotic form for values of $r\lesssim t$. It is also interesting to contrast the relatively greater weighting of large r values for $M_1^1(r,t=1)$, $b=10$ (Fig. 6) with the concentration of $M_1^0(r,t=1)$, $b=10$ around $t=0$ (Fig. 3).

The general conclusion that follows from these comparisons for these $l=1$ multipoles is that the asymptotic approximation agrees very well with exact calculations for $\gamma=200$ and 20 000. Even for $\gamma=10$ agreement is good for $b=1$ and fair for $b=10$. As we will see below, $b=10$ is an impact parameter already into the perturbative regime.

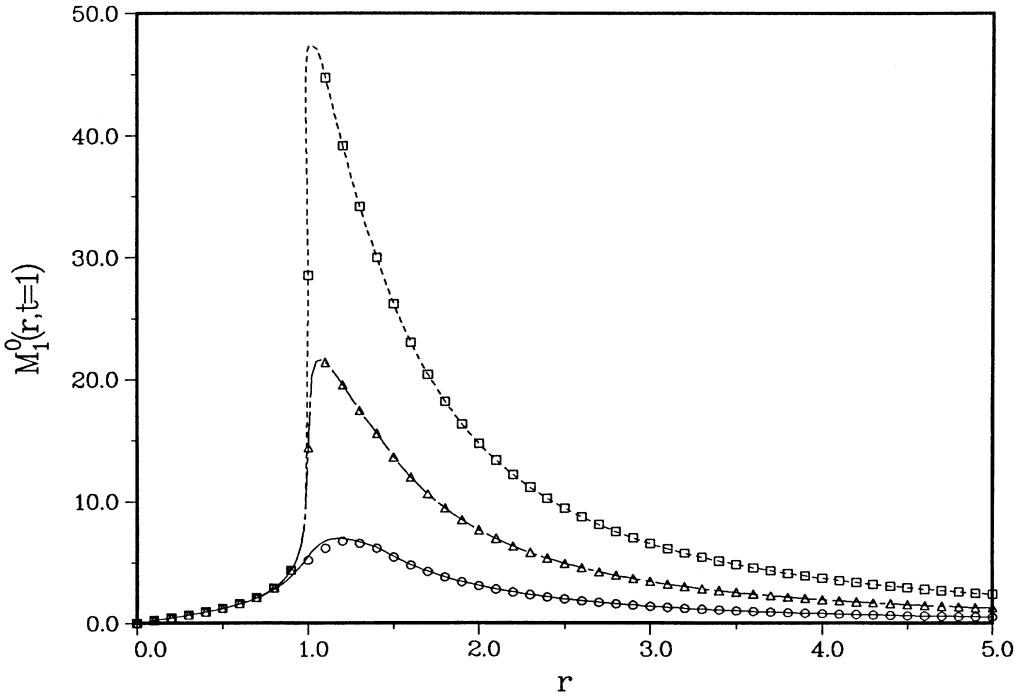

FIG. 1. Graph of the radial dependence of M_1^0, the scalar multipole defined generally in Eq. (2.2), for ($l=1$, $m=0$) and the choice of variables ($t=1$, $b=1$). Units of length are ($\hbar/m_e c$), and units of time are ($\hbar/m_e c^2$). The code for the plotted calculations of Figs. 1–6 is as follows: solid line: $\gamma=10$, exact form; circles: $\gamma=10$, asymptotic form; long-dashed-dotted line: $\gamma=200$, exact form; triangles: $\gamma=200$, asymptotic form; short-dashed line: $\gamma=20\,000$, exact form; squares: $\gamma=20\,000$, asymptotic form.

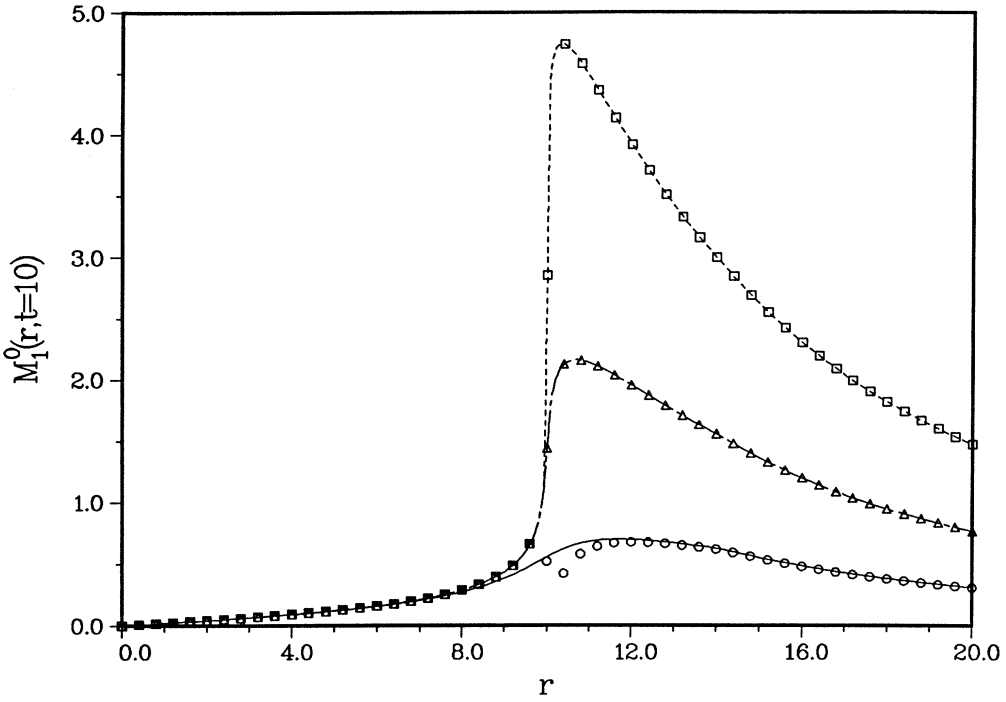

FIG. 2. M_1^0, $t=10$, $b=10$.

It is expected that higher multipole transitions will play a role in the nonperturbative region of small impact parameter. We have chosen one example ($l=10$, $m=0$) to illustrate the scalar multipole and its asymptotic form for a significantly higher angular momentum. Simple estimates, such as those presented in Sec. V, indicate that transitions should be negligible at an angular momentum value an order of magnitude larger than 10. We consider this example as providing a large enough value of l to exhibit large l characteristics, but small enough to be physically relevant.

Figures 7 and 8 show the ($l=10$, $m=0$) multipole for

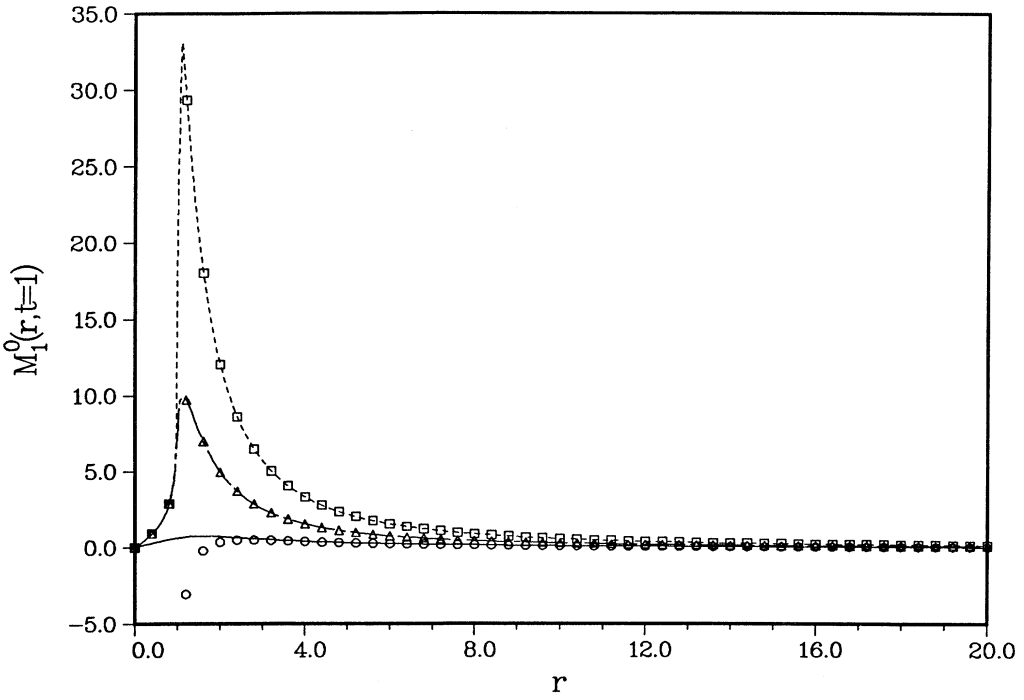

FIG. 3. M_1^0, $t=1$, $b=10$.

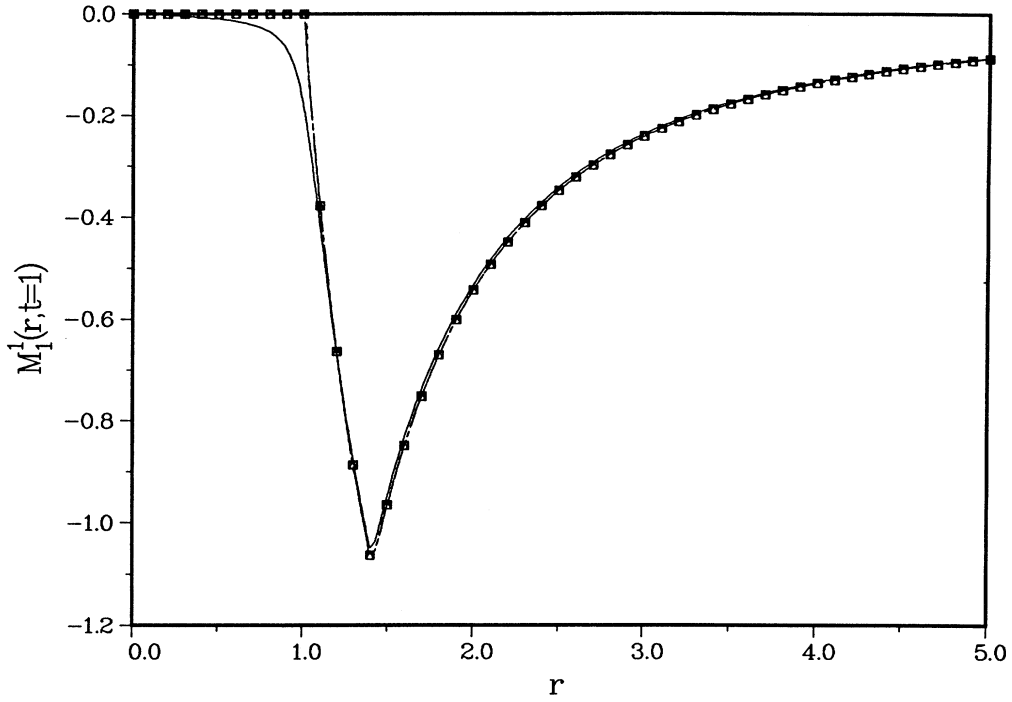

FIG. 4. M_1^1, $t=1$, $b=1$.

$b=1$, $t=1$, and for the γ values of 10 and 200. At γ of 10 the asymptotic form fails miserably, as is evident from Fig. 7. The solid line, representing the exact calculation, is quite reliable: The two independent methods of performing the exact calculation agree to about one-half of 1% or better. The reason why the discrepancy here between the exact (line) and asymptotic (circles) calculations is so much larger than for the ($l=1$, $m=0$) case (Fig. 1) is the $[(l+1)(l+2)]$ weighting that appears in the order $1/\gamma^2$ term; the relative correction is $\sim(b^2/t^2)(1/\gamma^2)(l+1)(l+2)/2$.

For the larger γ value of 200 the agreement between

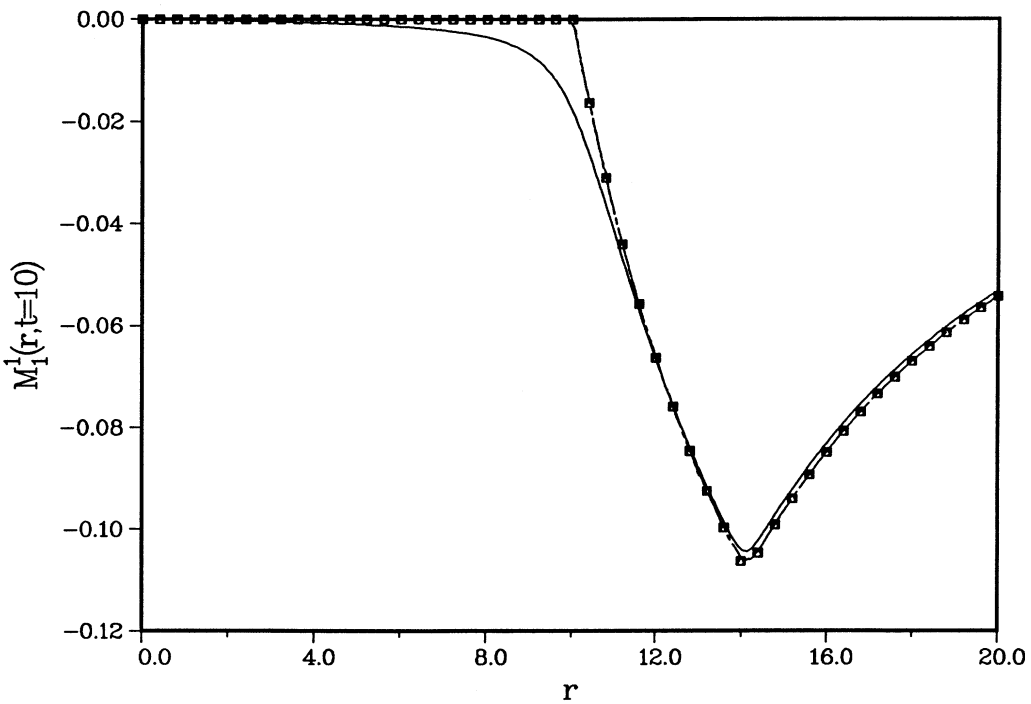

FIG. 5. M_1^1, $t=10$, $b=10$.

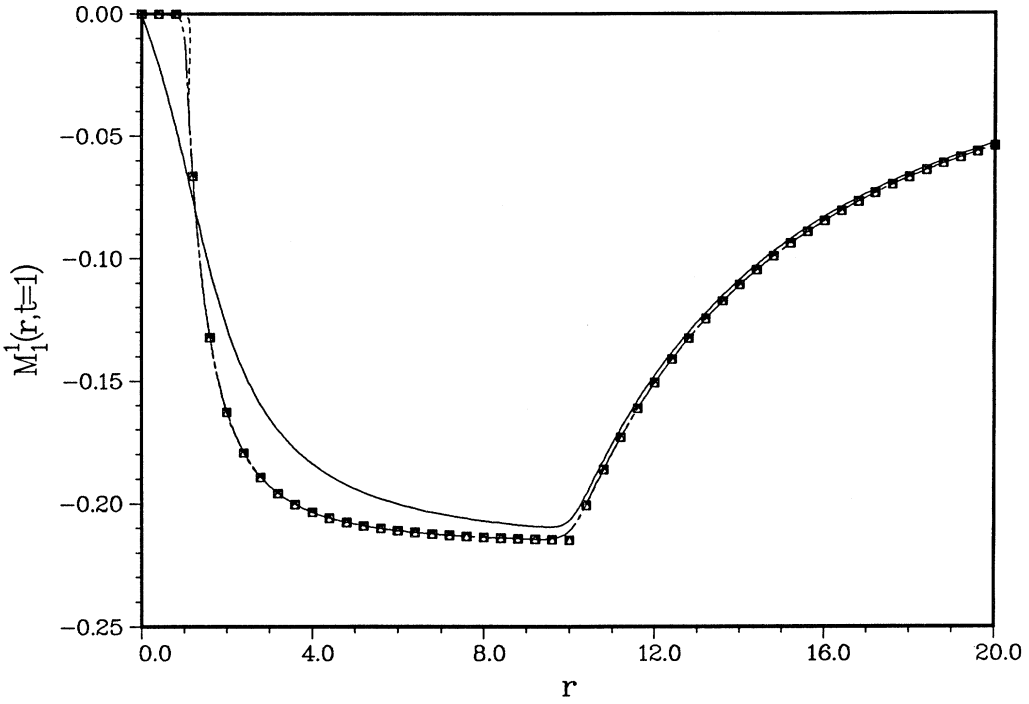

FIG. 6. M_1^1, $t=1$, $b=10$.

the asymptotic and exact calculations has returned as is evident in Fig. 8. The oscillating pattern simply reflects the $P_l(t/r)$ of the asymptotic form for $r>t$. The last zero of the multipole is hardly visible on the scale of the plot but occurs at $r=6.73$. For $\gamma=200$ at $r>(b^2+t^2)^{1/2}$ agreement between the asymptotic form and the exact formulation of the multipole decomposition, Eq. (3.5), is better than one part in 10^3. At $r=1.1$ the three methods have a mutual deviation of 1–2 %. At the singular point itself, $r=1$ (see Fig. 8), the deviation is tens of percent; recall, however, the integrability argument outlined in connection with Eq. (2.10). At the lowest values of r the

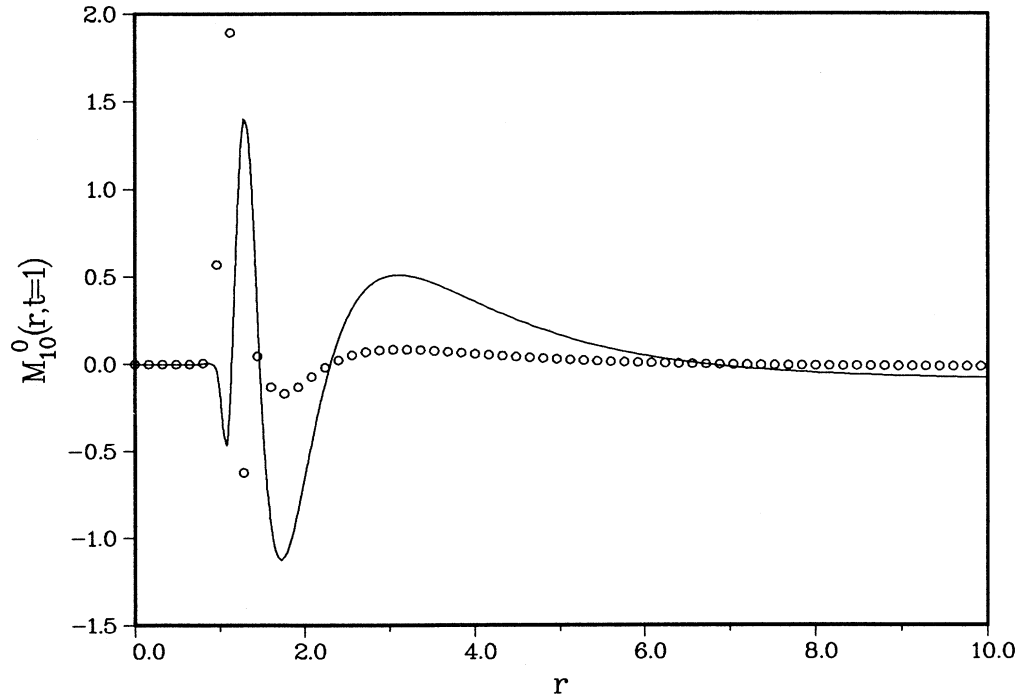

FIG. 7. Calculated scalar multipole M_{10}^0 ($l=10$, $m=0$), $t=1$, $b=1$, $\gamma=10$. Solid line, exact form; circles, asymptotic form.

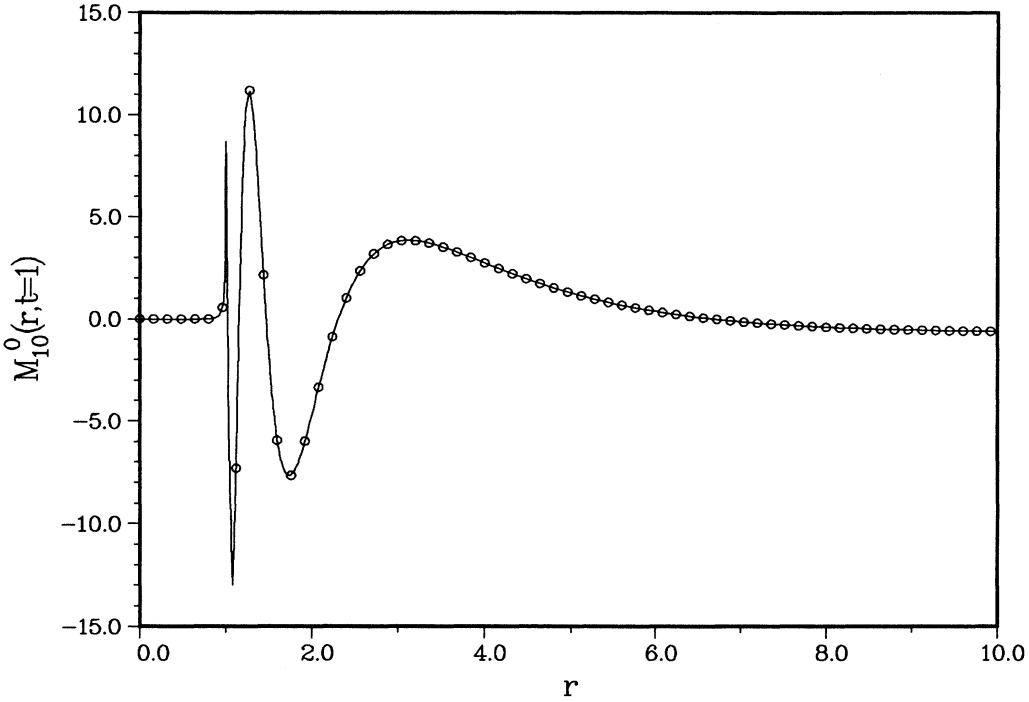

FIG. 8. M^0_{10}, $b=1$, $\gamma=200$.

values of the scalar multipole become so small that the exact methods are inadequate. However, since the values are so very small, their exact evaluation is unimportant. The situation for $\gamma=20\,000$ is similar to that for $\gamma=200$, except that the agreement between the asymptotic form and the exact multipole form is better than about one part in 10^6 rather than one part in 10^3 for $r>(b^2+t^2)^{1/2}$. However, the numerical integration differs from both as much as 2% because of the limited number of mesh points.

IV. GAUGE TRANSFORMATIONS

The basic problem is the solution of the Dirac equation:

$$\frac{i\partial\psi}{\partial t}=[H_0+V_p(t)]\psi=H(t)\psi \ .$$

The H_0 consists of the kinetic energies of the electron field and the Coulomb interaction with the target ion. For the immediate application to a high-Z target it is a sufficient approximation to drop the interactions between electrons, and, therefore, to reduce the problem to a sum of one-body problems, whose solution is to be written as an antisymmetrized product wave function. In what follows it is not strictly necessary to use this one-body assumption, but since it is conceptually simpler and necessary for practical calculations we adopt it.

A gauge transformation is effected by writing

$$\psi=e^{-i\chi(\mathbf{r},t)}\psi' \ , \tag{4.1}$$

to obtain

$$\frac{i\partial\psi'}{\partial t}=\left[H(t)-\frac{\partial\chi}{\partial t}-\boldsymbol{\alpha}\cdot\nabla\chi\right]\psi' \ . \tag{4.2}$$

The use of

$$\chi_1=(2\ln 2\gamma)\alpha Z_p\theta(z-t) \tag{4.3}$$

[$\theta(x)$ is the usual step function] then removes the γ-dependent part of the interaction

$$(2\ln 2\gamma)\alpha Z_p(1-\alpha_z)\delta(z-t) \ . \tag{4.4}$$

This then completes the promised removal of the explicit γ dependence.

We can, however, do even better, and remove the $\ln b$ dependence that remains for the large-b region ($r<[b^2+(v_pt)^2]^{1/2}$), replacing it with terms that manifestly fall at least as $1/b$. This replacement is important in order to establish the weakness of the interaction in this large-b domain, and, thereby, the connection to the perturbational results. The useful choice of the gauge transformation (we put off the motivation for this choice until later in this section) is

$$\chi_2=-\frac{\alpha Z_p}{v_p}\ln\frac{\gamma(z-v_pt)+[\gamma^2(z-v_pt)^2+b^2]^{1/2}}{(z-v_pt)+[(z-v_pt)^2+b^2]^{1/2}} \ , \tag{4.5}$$

which then adds to the interaction $V_p(t)$

$$\frac{-\alpha Z_p[1-(1/v_p)\alpha_z]}{[(z-v_pt)^2+b^2/\gamma^2]^{1/2}}+\frac{\alpha Z_p[1-(1/v_p)\alpha_z]}{[(z-v_pt)^2+b^2]^{1/2}} \ . \tag{4.6}$$

The multipole decomposition of the first term is very similar to that carried out for $V_p(t)$, except that there are only $m=0$ terms to consider (since there is no ρ dependence); in fact, the results are just the negative of those obtained except for the absence of the term involving the factor $\theta((r^2-(v_pt)^2)/b^2-1)$. The gauge subtraction will then remove all except the negative of this term, leaving us with (to order $\ln\gamma/\gamma^2$) the $m\neq 0$ terms of Eq. (2.9) and

$$\alpha Z_p(1-v_p\alpha_z)\sum_l Y_l^0(\theta)\frac{\sqrt{\pi}\sqrt{2l+1}}{r}P_l\left[\frac{v_pt}{r}\right]\times\begin{cases}0 & \text{if } r<|v_pt|\\ 0 & \text{if } |v_pt|<r<[b^2+(v_pt)^2]^{1/2}\\ -\ln\dfrac{r^2-(v_pt)^2}{b^2} & \text{if } r>[b^2+(v_pt)^2]^{1/2}\end{cases}$$
$$+\alpha Z_p\left[1-\frac{1}{v_p}\alpha_z\right]\sum Y_l^0(\theta)\int d\Omega'\frac{Y_l^0(\theta')}{[(z-v_pt)^2+b^2]^{1/2}}\ . \tag{4.7}$$

The last term, brought in by the gauge transformation, is obviously independent of γ, vanishes at least as fast as $1/b$ at large values of b, and is easy to evaluate analytically by elementary integration for each l value. The net result of this second gauge transformation is a highly compact interaction with no γ dependence, which weakens with increasing impact parameter at least as fast at $1/b$, and which permits a very simple multipole expansion.

The paper of Toshima and Eichler [10] proposes and illustrates the use of a transform similar to the γ-dependent term of Eq. (4.5) to solve the important difficulty in calculations with interactions that drop off as slowly as $1/t$ [such as the $l=0$, $m=0$ term in Eq. (2.9)].

In order to clearly and definitively establish a connection with the familiar Weizsacker-Williams approximation, which offers a convenient form of perturbation theory, we present a third gauge transformation. This χ_3 is chosen so as to transform the scalar part of $V_p(t)$ to the instantaneous Coulomb interaction, following the classic Fermi strategy designed to display the transverse modes. That is, χ_3 is defined to satisfy

$$\frac{\alpha Z_p}{\{[(\mathbf{b}-\boldsymbol{\rho})/\gamma]^2+(z-v_pt)^2\}^{1/2}}-\frac{\partial\chi_3}{\partial t}=\frac{\alpha Z_p}{[(\mathbf{b}-\boldsymbol{\rho})^2+(z-v_pt)^2]^{1/2}}\ , \tag{4.8}$$

thereby leading to

$$\chi_3=-\frac{\alpha Z_p}{v_p}\ln\frac{(z-v_pt)+\{[(\mathbf{b}-\boldsymbol{\rho})/\gamma]^2+(z-v_pt)^2\}^{1/2}}{(z-v_pt)+[(\mathbf{b}-\boldsymbol{\rho})^2+(z-v_pt)^2]^{1/2}}\ . \tag{4.9}$$

The resultant interaction is

$$\frac{\alpha Z_p}{v_p}\left[\frac{-\boldsymbol{\alpha}\cdot(\mathbf{b}-\boldsymbol{\rho})}{|\mathbf{b}-\boldsymbol{\rho}|^2}\right]\left[\frac{z-v_pt}{\{[(\mathbf{b}-\boldsymbol{\rho})/\gamma]^2+(z-v_pt)^2\}^{1/2}}-\frac{z-v_pt}{[(\mathbf{b}-\boldsymbol{\rho})^2+(z-v_pt)^2]^{1/2}}\right]$$
$$+\frac{\alpha Z_p(1-\alpha_z/v_p)}{[(\mathbf{b}-\boldsymbol{\rho})^2+(z-v_pt)^2]^{1/2}}-\frac{1}{\gamma^2}\frac{\alpha Z_p\alpha_z/v_p}{\{[(\mathbf{b}-\boldsymbol{\rho})/\gamma]^2+(z-v_pt)^2\}^{1/2}}\ . \tag{4.10}$$

The last term is explicitly of order $1/\gamma^2$, and so is to be dropped. The first, the transverse terms, can be well approximated either by the formal analysis used above, or, more simply, by noting that the γ dependence can only be important (for b,ρ confined as before) for $(z-v_pt)\sim 0$, where, however, the numerator vanishes. This leaves us with the approximation to order $\ln\gamma/\gamma^2$:

$$\alpha Z_p\left[\frac{-\boldsymbol{\alpha}\cdot(\mathbf{b}-\boldsymbol{\rho})}{|\mathbf{b}-\boldsymbol{\rho}|^2}\right]\left[\frac{z-t}{|z-t|}-\frac{z-t}{[(\mathbf{b}-\boldsymbol{\rho})^2+(z-t)^2]^{1/2}}\right]+\frac{\alpha Z_p(1-\alpha_z)}{[(\mathbf{b}-\boldsymbol{\rho})^2+(z-t)^2]^{1/2}} \tag{4.11}$$

Again, the γ dependence has disappeared to order $\ln\gamma/\gamma^2$. The importance of the transverse components is manifest; the scalar plus longitudinal term is of order 1 and must be kept, although, as shown in Sec. V, its contribution vanishes in lowest-order perturbation theory.

In order to connect with the region of large impact parameters, we will return to the full form (4.10), and use it in Sec. V to obtain the Weizsacker-Williams approximation to perturbation theory.

These gauge transformations that extinguish the explicit γ dependence, up to higher orders in $1/\gamma$, are realizations of the qualitative statement that compression of the longitudinal dimensions has produced such a very sharp pulse that the precise shape cannot matter. However,

this angular compression, $\sim 1/\gamma$, means that at large impact parameters, say $\gamma\hbar/m_e c$, the linear spreads are of order $\hbar/m_e c$—the scale of interest to us—and the γ independence is no longer maintained. As will be seen explicitly in the perturbation theory of Sec. V, there is a sharp dropoff in the strength of the interaction at $\sim\gamma\hbar/m_e c$, which indeed provides the cutoff required for the cross section to be finite.

Before leaving the subject of gauge transforms, it is important to examine the effects on the initial boundary conditions and the final values of the wave function. Should χ have other than constant values at these limits the input and output might well be in a transformed basis quite different from the physical form one has in mind. As we shall see, this complication is absent from all three gauge transforms considered here.

In the present problem the boundary conditions are placed at $t=-\infty$ and the results read out at $t=+\infty$. How does χ_1 behave? At $t=-\infty$, the step function is constant for all $z>-\infty$; at $t=+\infty$ it vanishes for all $z<+\infty$; this gauge transform then changes the chosen, physical basis only by a constant phase factor at the physical input/output points. The χ_2 and χ_3 are somewhat less obvious to see through. However, it is easily seen that for finite spatial parameters

$$\lim_{t\to-\infty}\chi_{2,3}\to\frac{-\alpha Z_p}{v_p}\ln\gamma\ ,\quad \lim_{t\to+\infty}\chi_{2,3}\to\frac{-\alpha Z_p}{v_p}\ln 1/\gamma\ , \tag{4.12}$$

and again the basis is transformed only to the extent of a constant phase factor. Of course, in any numerical calculation the time dependence must be taken far enough to ensure asymptotia. These gauge transforms, then, complete the task of showing that the cross section for bound-electron–positron pair production at $b\ll\gamma\hbar/m_e c$ is independent of γ (to order $1/\gamma$ or higher).

There is always the standard question of the completeness of the basis in which a calculation is performed; one must be certain that any incompleteness does not spoil the connection between the transformed and untransformed wave functions spelled out in Eqs. (4.1) and (4.2). To make this explicit, suppose that the solution of

$$\frac{i\partial\psi}{\partial t}=H\psi$$

is sought, as has been much the case, via a coupled-channels format:

$$\begin{aligned}\psi&=\sum_m e^{-iE_m t}\phi_m(\mathbf{r})a_m(t)\ ,\\ \frac{i\partial a_n}{\partial t}&=\sum_m e^{i(E_n-E_m)t}\langle n|V_p(t)|m\rangle a_m(t)\ ,\end{aligned} \tag{4.13}$$

where the ϕ_m are the (possibly limited) set of eigenfunctions of H_0. In the gauge transformed problem, with the interaction now

$$V_p(t)-\frac{\partial\chi}{\partial t}-\boldsymbol{\alpha}\cdot\nabla\chi\ , \tag{4.14}$$

use of the function

$$\psi'=\sum_k e^{-iE_k t}e^{i\chi}\phi_k(r)a_k'(t) \tag{4.15}$$

leads to the time-dependent equation

$$ie^{i\chi}\sum_k e^{-iE_k t}\phi_k(r)\frac{\partial a_k'}{\partial t}=e^{i\chi}V_p(t)\sum_l e^{-iE_l t}\phi_l(r)a_l'(t)\ , \tag{4.16}$$

the χ-dependent terms of the interaction having been canceled off. Projection with the possibly delimited basis states then results in equations for the a_k' set of precisely the same form as those for the a_m set. Finally, since the χ function approaches a constant value at $t=-\infty$ and another constant at $t=+\infty$, it is guaranteed that the physical input/output conditions are invariant. This holds whether or not the basis set is complete, subject only to the obvious demand that the basis set be the same in the two gauge conditions.

Should the question of gauge invariance be posed in another more usual way, the lack of completeness might well be harmful. If instead of the expansion (4.15) for the ψ' function, a straightforward decomposition in the basis set in usage is put forward,

$$\psi'=\sum_k e^{-iE_n t}\phi_n(\mathbf{r})b_n(t)\ , \tag{4.17}$$

the relation between the b's and the a's is no longer trivial. The paper of Rumrich and Greiner [11] examines how invariance is spoiled by an incomplete basis. An ameliorative reformulation of coupled channels by Kobe and Kennedy [12] provides one means for the provision of explicit gauge invariance within a truncated basis, but at the expense of a time-dependent basis set.

V. THE PERTURBATIVE REGION

The probability of a transition states 0 and f is given in lowest order by the usual form:

$$\begin{aligned}P_{0f}&=\rho_f|a_{0f}|^2\ ,\\ a_{0f}&=\frac{1}{i}\int\psi_f^*(r)V_p(\mathbf{r},t)\psi_0(\mathbf{r})e^{i(E_f-E_0)t}d\tau\,dt\ .\end{aligned} \tag{5.1}$$

The time integration is immediately given by the Fourier integral of $V_p(\mathbf{r},t)$. With the gauge choice leading to the interaction of Eq. (4.10) and the well-known integral expressions of the modified Bessel functions,

$$\begin{aligned}\int_{-\infty}^{\infty}dx\frac{x}{(\beta^2+x^2)^{1/2}}e^{i\omega x}&=2i|\beta|K_1(|\omega\beta|)\left[\frac{\omega}{|\omega|}\right]\ ,\\ \int_{-\infty}^{\infty}dx\frac{1}{(\beta^2+x^2)^{1/2}}e^{i\omega x}&=2K_0(|\omega\beta|)\ ,\end{aligned} \tag{5.2}$$

the first-order amplitude is

$$a_{0f}=-\frac{2\alpha Z_p}{v_p^2}\int d\tau\,\psi_f^*(\mathbf{r})\frac{\boldsymbol{\alpha}\cdot(\mathbf{b}-\boldsymbol{\rho})}{|\mathbf{b}-\boldsymbol{\rho}|^2}\psi_0(\mathbf{r})e^{i\omega z}\left|\left|\frac{\mathbf{b}-\boldsymbol{\rho}}{\gamma}\right|K_1\left|\left|\left[\frac{\mathbf{b}-\boldsymbol{\rho}}{\gamma}\right]\omega\right|\right|-|\mathbf{b}-\boldsymbol{\rho}|K_1(|(\mathbf{b}-\boldsymbol{\rho})\omega|)\right]\frac{\omega}{|\omega|}$$
$$+\frac{2\alpha Z_p}{v_p^2}\frac{1}{i}\int d\tau\,\psi_f^*(\mathbf{r})\left[1-\frac{\alpha_z}{v_p}\right]\psi_0(\mathbf{r})e^{i\omega z}K_0(|(\mathbf{b}-\boldsymbol{\rho})\omega|)+\frac{2\alpha Z_p}{v_p^2}\frac{1}{\gamma^2}\int d\tau\,\psi_f^*(\mathbf{r})\alpha_z\psi_0(\mathbf{r})e^{i\omega z}K_0\left|\left|\frac{\mathbf{b}-\boldsymbol{\rho}}{\gamma}\omega\right|\right|,$$
$$\omega=(E_f-E_0)/v_p\ . \tag{5.3}$$

At large values of the impact parameter $b\gg\rho$, and a_{0f} can be simplified by dropping the ρ dependence:

$$a_{0f}\simeq-\frac{2\alpha Z_p}{v_p^2}\left[\int d\tau\,\psi_f^*(\mathbf{r})\boldsymbol{\alpha}\cdot\hat{\mathbf{b}}\psi_0(\mathbf{r})e^{i\omega z}\right]\left[\frac{1}{\gamma}K_1\left|\left|\frac{b\omega}{\gamma}\right|\right|-K_1(|b\omega|)\right]\frac{\omega}{|\omega|}$$
$$+\frac{2\alpha Z_p}{v_p^2}\frac{1}{i}\left[\int d\tau\,\psi_f^*(\mathbf{r})\left[1-\frac{\alpha_z}{v_p}\right]\psi_0(r)e^{i\omega z}\right]K_0(1-O(p/b))(|b\omega|)+\frac{2\alpha Z_p}{v_p^2}\frac{1}{\gamma^2}\left[\int d\tau\,\psi_f^*(r)\alpha_z\psi_0 e^{i\omega z}\right]K_0\left|\left|\frac{b\omega}{\gamma}\right|\right|. \tag{5.4}$$

The last term is clearly of order $\ln\gamma/\gamma^2$ since $K_0(z)$ is $\sim(-\ln z)$ for $z\ll1$, and drops as $(\pi/2z)^{1/2}e^{-z}$ for $z\gg1$. The main part of the second term simply vanishes, but requires some manipulation for this to be easily seen; application of the current conservation relation

$$\int d\tau\,\psi_f^*\frac{\alpha_z}{v_p}e^{i\omega z}\psi_0=\frac{1}{\omega v_p}\int d\tau\,\psi_f^*[H_0,e^{i\omega z}]\psi_0$$
$$=\int d\tau\,\psi_f^*e^{i\omega z}\psi_0 \tag{5.5}$$

guarantees the cancellation between the two parts. A similar treatment cancels the $K_1(b\omega)$ term.

The remaining, first term is the sole contributor to leading order:

$$P_{0f}(b)=4(\alpha Z_p)^2\rho_f\left|\int d\tau\,\psi_f^*\boldsymbol{\alpha}\cdot\hat{\mathbf{b}}\psi_0e^{i\omega z}\right|^2$$
$$\times\left[\frac{1}{\gamma}K_1\left|\left|\frac{b\omega}{\gamma}\right|\right|\right]^2. \tag{5.6}$$

The matrix element is immediately seen to closely approximate that which governs photon absorption; the transverse nature of the operator is manifest, and the connection between energy and momentum transfer, $\omega=(E_f-E_0)/v_p$, approaches that of the photon as $v_p\to1$, differing only to $O(1/\gamma^2)$. Recalling that the photon cross section is

$$\sigma_{\rm ph}(\omega)=\frac{(2\pi)^2}{\omega}\alpha\rho_f\left|\int d\tau\,\psi_f^*\boldsymbol{\alpha}\cdot\hat{\mathbf{e}}\psi_0e^{i\omega z}\right|^2 \tag{5.7}$$

allows us to write P_{0f} to order $1/\gamma^2$, in terms of $\sigma_{\rm ph}$. Then the integrated (over ω) probability as a function of impact parameter $P(b)$ is

$$P(b)=\int d\omega\,P_{0f}$$
$$=\frac{\alpha Z_p^2}{\pi^2}\int d\omega\,\omega\sigma_{\rm ph}(\omega)\left[\frac{1}{\gamma}K_1\left|\left|\frac{b\omega}{\gamma}\right|\right|\right]^2. \tag{5.8}$$

While it is easy to work with the b dependence of the modified Bessel functions, it is clarifying to look at the large-γ limits. As we shall see below, the b region appropriate for perturbative calculations is $b\gtrsim5\hbar/m_ec$, and, of course, $\omega\gtrsim2m_ec^2$, so that $b\omega>10$. Since $K_1(z)\simeq1/z+O(z)$ for z small, and drops faster than exponentially [as $(\pi/2z)^{1/2}e^{-z}$] for $z\gg1$, we see that

$$\left[\frac{1}{\gamma}K_1\left|\left|\frac{b\omega}{\gamma}\right|\right|\right]\simeq\frac{1}{b|\omega|} \tag{5.9}$$

for the region $10<b|\omega|<\gamma$, and drops rapidly as $(b|\omega|)>\gamma$. This immediately shows the $1/b^2$ behavior of $P(b)$, as is appropriate for an interaction falling as $1/b$. It is important to note that had we started with the asymptotic approximation to the gauge transformed interaction, Eq. (4.11), the

$$\left|\left|\frac{\mathbf{b}-\boldsymbol{\rho}}{\gamma}\right|\right|K_1\left|\left|\left[\frac{\mathbf{b}-\boldsymbol{\rho}}{\gamma}\right]\omega\right|\right|$$

of Eq. (5.4) would have been replaced by $1/|\omega|$ leaving us with the result just obtained. However, as the impact parameter becomes very large, $O(\gamma\hbar/m_ec)$, the asymptotic forms are no longer applicable, and the exact expressions are needed, as in calculating a total perturbative cross section:

$$\sigma_{\rm pert}=\int d^2b\,P(b)$$
$$=\frac{2}{\pi}\alpha Z_p^2\int d\omega\,\omega\sigma_{\rm ph}(\omega)$$
$$\times\int_{b_{\rm min}}^{\infty}db\,b\left[\frac{1}{\gamma}K_1\left|\left|\frac{b\omega}{\gamma}\right|\right|\right]^2. \tag{5.10}$$

Here $b_{\rm min}$ is to be chosen so as to justify (1) the validity of perturbation theory, (2) dropping the ρ dependence, and (3) a smooth connection with the nonperturbative calculations for $b\le b_{\rm min}$.

The final evaluation of σ_{pert} involves a straightforward integration over the impact parameter dependence. The details are left to the Appendix; the result is, to $O(\ln\gamma/\gamma^2)$,

$$\sigma_{\text{pert}} \simeq \frac{2}{\pi}\alpha Z_p^2 \int d\omega \frac{1}{\omega}\sigma_{\text{ph}}(\omega)\ln\frac{\gamma}{(0.89)\omega b_{\min}} \ ; \quad (5.11)$$

small terms, of order $(\pi/2\omega b_{\min}^{1/2}e^{-\omega b_{\min}}) < 2\times 10^{-5}$ have been dropped. It is important to note that the $\ln\gamma$ dependence comes about not through a γ dependence of $P(b)$, but rather through the accumulation of probabilities over a large range of impact parameters, up to an order of $\gamma\hbar/m_e c$.

The comparison between the asymptotic limit and the exact form of the interaction, noted above, also affords an additional assessment of the validity of the asymptotic approximation. The frequency response of the exact interaction is governed by

$$\left|\frac{\mathbf{b}-\boldsymbol{\rho}}{\gamma}\right| K_1\left(\left|\left[\frac{\mathbf{b}-\boldsymbol{\rho}}{\gamma}\right]\omega\right|\right) ,$$

while the asymptotic forms result in $1/|\omega|$. The physical explanation is easily seen. The frequency response at ω is determined by the spatial conjugate variable $(z-v_p t)$. At values smaller than $|(\mathbf{b}-\boldsymbol{\rho})/\gamma|$, the variability of the interaction as a function of $(z-v_p t)$ falls off, thereby producing the cutoff at $|(\mathbf{b}-\boldsymbol{\rho})/\gamma\omega| \gtrsim 1$. In the present problem concerning bound-state population, perturbation theory tells us that excitation energies above some $20m_e c^2$ are not important; then, for $|\mathbf{b}-\boldsymbol{\rho}| \lesssim \gamma/20(\hbar/m_e c)$ the asymptotic approximation will do. A $\gamma \gtrsim 200$ permits the small-b nonperturbative calculation to use the asymptotic simplifications.

In deciding on a safe bound within which perturbative estimates are valid it is prudent to base oneself on smallness of the rates for the strongest modes that might enter on a physical or virtual basis. For the present problem of bound-electron–positron pair creation, one of the very strong interacting modes is the sweepoff of a bound K electron by the transiting ion. Simple estimates [2] based on perturbation values indicate an integrated probability for this mode of $\sim 1.5(b/\hbar/m_e c)^{-2}$. This points to a domain $b > 5\hbar/m_e c$ within which estimates based on the Weizsacker-Williams approximation would be valid, and connection with a full coupled-channel set could then be made at the boundary.

Having decided to use perturbation theory for $b \gtrsim 5\hbar/m_e c$, we now apply Eq. (5.11) to the specific mode of bound-electron–positron pair formation. The photon cross section falls off with increasing ω sufficiently quickly so that the integral converges and σ_{pert} takes the form

$$A\ln\gamma + B_p \quad (5.12)$$

where both A and B_p are independent of γ to within higher orders in $1/\gamma$, A has been calculated to be 7.80 ± 0.06 b for fully stripped Au+Au; more generally for $Z+Z$, there is a Z^x dependence, x between 7 and 8.5 for Z between 14 and 80; B contains a weak dependence on $b_{\min}$, which we now take as $\sim 5\hbar/m_e c$. To this perturbation contribution the nonperturbative contributions that come from impact parameters smaller than $b_{\min}$ must be added; but these inner contributions we have shown by explicit gauge transformations to be independent of γ (to within higher order in $1/\gamma$). The net result is the prediction that the total cross section for bound-electron–positron production is of the form

$$A\ln\gamma + B \ , \quad (5.13)$$

with A as given above, and both A and B independent of ion energy up to higher orders in the small parameter $1/\gamma$.

This strong conclusion means that experiments at reasonably large values of γ (say 200) can be used to predict results at $\gamma \sim 2\times 10^4$ or higher. Again, attention is called to the weak, logarithmic, dependence of the cross section on energy; even large energy jumps are only short extrapolations.

VI. DISCUSSION OF A DIFFICULTY WITH INTERPRETATION OF EXPERIMENTS

Regrettably, the use of fixed targets means that only the projectile ion can be fully stripped; the strength of the interaction acting on it is weakened by screening. Because the $\ln\gamma$ term of the perturbative contribution comes about from addition over a large range of impact parameters up to $\sim\gamma\hbar/m_e c$, the screening effects can be significant. Thus, since bound state radii are $\sim(n\hbar/m_e c)(1/\alpha Z)$, screening effects in the case of Au+Au begin at impact parameters of a few multiples of $\hbar/m_e c$, and so effect a fraction of the parameter region that results in the $\ln\gamma$ term. A rough estimate of the screening effect can be obtained by assuming the effective target charge seen by the stripped projectile ion is the screened Thomas-Fermi value evaluated at the distance of closest approach. With the approximate form $Z_{\text{eff}} = Ze^{-b/a}$, the perturbative value is changed by a ratio of order

$$\sim \int_{b_{\min}}^{\gamma/\omega} e^{-2b/a}\frac{1}{b}db \Big/ \int_{b_{\min}}^{\gamma/\omega}\frac{1}{b}db$$

where $a = (\hbar/m_e c)/\alpha Z^{1/3}$. ω is some representative energy, which we take as $3m_e c^2$. For an Au target, this amounts to $\sim\frac{1}{3}$ at $\gamma = 200$ and $b_{\min} = 5\hbar/m_e c$. (Note that at low values of γ, say $\gamma = 10$, $\omega b_{\min} > \gamma$, and there is no real perturbative region.) Detailed screening calculations will be necessary to adequately match experimental determinations. Ignoring the entire contribution of the large-b region and attributing the entire experimental cross section to the small impact parameter region would provide an overestimate of the latter's contribution. Adding this together with the perturbative contribution might provide a possibly useful bound for the collider, fully stripped cross section.

APPENDIX A

In this appendix some of the details of the integrals or expansions that may be less familiar are shown.

(i) The integral that appears in Eq. (2.5a),

$$\mathcal{I}_l=\int_\alpha^1 dx\frac{P_l(x)-P_l(\alpha)}{x-\alpha}+\int_{-1}^\alpha dx\frac{P_l(x)-P_l(\alpha)}{\alpha-x}\ ,$$

is clearly expressible as a sum of polynomials, since the $P_l(x)$'s are such and the integrands can then be written as powers of $(x-\alpha)$. The first few l values are trivially evaluated:

$$\mathcal{I}_0=0,\quad \mathcal{I}_1=-2P_1(\alpha)\ ,$$
$$\mathcal{I}_2=-3P_2(\alpha),\quad \mathcal{I}_3=-\tfrac{11}{3}P_3(\alpha)\ ;$$

these strongly suggest the general result

$$\mathcal{I}_l=\left[-2\sum_{n=1}^{l}\frac{1}{n}\right]P_l(\alpha)\ ,$$

which is easily proved by induction. First, a recursion relation for the $\mathcal{I}_l$'s is easily constructed using the familiar one for the Legendre polynomials

$$P_l(x)=\frac{2l-1}{l}xP_{l-1}(x)-\frac{l-1}{l}P_{l-2}(x)\ ,$$

$$\mathcal{I}_l=\frac{2l-1}{l}\alpha\mathcal{I}_{l-1}-\frac{l-1}{l}\mathcal{I}_{l-2}+\frac{2l-1}{l}\left[\int_\alpha^1 dx'P_{l-1}(x')+\int_\alpha^{-1}dx'P_{l-1}(x')\right];$$

recalling that

$$P_{l-1}(x)=\frac{1}{2l-1}\frac{d}{dx}[P_l(x)-P_{l-2}(x)]$$

puts the recursion relation in compact form

$$\mathcal{I}_l=\frac{2l-1}{l}\alpha\mathcal{I}_{l-1}-\frac{l-1}{l}\mathcal{I}_{l-2}-\frac{2}{l}[P_l(\alpha)-P_{l-2}(\alpha)]\ .$$

The inductive proof is then a matter of straightforward insertion of the conjectured form for $\mathcal{I}_{l-1}$, $\mathcal{I}_{l-2}$ to find the conjectured form valid for $\mathcal{I}_l$.

(ii) The integral over the impact parameter used to obtain Eq. (5.11) is based on two indefinite integrals of modified Bessel functions taken from Luke [13], Sec. 11.2:

$$\int^z tK_1(kt)K_1(kt)dt$$
$$=(z^2/2)[K_1^2(kz)-K_0(kz)K_2(kz)]$$
$$=(z^2/2)[K_1^2(kz)-K_0^2(kz)-(2/kz)K_0(kz)K_1(kz)]$$

and

$$\int^z tK_1(kt)K_1(lt)dt$$
$$=\frac{z}{k^2-l^2}[kK_2(kz)K_1(lz)-lK_1(kz)K_2(lz)]$$
$$=\frac{z}{k^2-l^2}[lK_1(kz)K_0(lz)-kK_0(kz)K_1(lz)]\ .$$

Then

$$\int_{b_{\min}}^\infty b\left[\frac{1}{\gamma}K_1\left[\frac{b\omega}{\gamma}\right]-K_1(b\omega)\right]^2db$$
$$=-\left\{\frac{1}{\gamma^2}\frac{b_{\min}^2}{2}\left[K_1^2\left[\frac{b_{\min}\omega}{\gamma}\right]-K_0^2\left[\frac{b_{\min}\omega}{\gamma}\right]-\frac{2\gamma}{\omega b_{\min}}K_0\left[\frac{b_{\min}\omega}{\gamma}\right]K_1\left[\frac{b_{\min}\omega}{\gamma}\right]\right]\right.$$
$$+\frac{b_{\min}^2}{2}\left[K_1^2(b_{\min}\omega)-K_0^2(b_{\min}\omega)-\frac{2}{\omega b_{\min}}K_0(b_{\min}\omega)K_1(b_{\min}\omega)\right]$$
$$\left.+\left[\frac{2}{\gamma}\right]\frac{\omega b_{\min}}{\omega^2-\omega^2/\gamma^2}\left[K_0(b_{\min}\omega)K_1\left[\frac{b_{\min}\omega}{\gamma}\right]-\frac{1}{\gamma}K_1(b_{\min}\omega)K_0\left[\frac{b_{\min}\omega}{\gamma}\right]\right]\right\}.$$

The large-γ limit is expressed by using the asymptotic expansions of K_1 and K_0 given by Abramowitz and Stegun [14],

$$K_n(z)=\sqrt{\pi/2z}\,e^{-z}\left[1+O\left[\frac{4n^2-1}{8z}\right]\right],\quad z\gg1$$
$$K_0(z)=-[\ln z/2+.5772...][1+O(z^2/4)]\ ,$$
$$K_1(z)=\frac{1}{z}[1+O(z^2/4)],\quad z\gg1\ .$$

(iii) The integral over the azimuthal angle used to obtain Eq. (2.7) is taken from Gradshteyn and Ryzhik [15], Sec. 4.397, Nos. 6, 7, 14, and 15.

(iv) The integral over the polar angle used in Eq. (2.5), which amounts to the definition of Q_l, is given in Sec. 7.224, No. 1 of Gradshteyn and Ryzhik [15]. The properties of the Q_l's, the Legendre functions of the second kind, are described in Secs. 8.82 and 8.83 of that volume, and, of course, in many other standard references.

(v) The integrals over spherical Bessel functions, Eqs. (3.3a) and (3.3b), are taken from Gradshteyn and Ryzhik [15], Sec. 6.574, Nos. 1, 2, and 3. The properties of the hypergeometric function $F(\alpha,\beta,\gamma,\delta)$ are described in Sec. 9.1 and in standard references.

[1] Brookhaven National Laboratory Report No. BNL 52195, 1989 (unpublished).

[2] Coverage of the subject can be found in two recent review articles: C. A. Bertulani and G. Baur, Phys. Rep. **163**, 299 (1988); J. Eichler, *ibid.* **193**, 165 (1990).

[3] M. Rhoades-Brown, C. Bottcher, and M. Strayer, Phys. Rev. A **40**, 2831 (1989). The cross sections for Au+Au, depicted in Fig. 2 of this reference, were based on the lowest order (in αZ_p) of perturbation theory; the final integrals were calculated via Monte Carlo evaluations, with the probable errors shown in the plot. The A coefficient discussed in the present work was extracted by fitting the linear dependence on $\ln\gamma$ to the cross-section values corresponding to $\gamma \gtrsim 17$, a value large enough to approach asymptotia. (Note that the γ used here, appropriate to a reference frame fixed on one of the ions, is related to that of the collider frame by $\gamma = 2\gamma_{\rm col}^2 - 1$.)

[4] Brookhaven National Laboratory Workshop Proceedings, Report No. BNL 52247, 1990 (unpublished).

[5] K. Momberger, N. Grün, W. Scheid, and U. Becker, J. Phys. B **23**, 2293 (1990); K. Rumrich, K. Momberger, G. Soff, W. Greiner, N. Grün, and W. Scheid, Phys. Rev. Lett. **66**, 2613 (1991).

[6] W. R. Johnson, D. J. Buss, and C. O. Carroll, Phys. Rev. **135A**, 1232 (1964).

[7] G. N. Watson, *Treatise on the Theory of Bessel Functions* (Cambridge University Press, London, 1958), Sec. 11.5, Eq. (9).

[8] G. Baker, *Essentials of Padé Approximates* (Academic, New York, 1975).

[9] P. Wynn, Numer. Math. **8**, 264 (1966).

[10] N. Toshima and J. Eichler, Phys. Rev. A **42**, 3896 (1990).

[11] K. Rumrich and W. Greiner, Phys. Lett. A **149**, 17 (1990).

[12] D. H. Kobe and P. K. Kennedy, J. Phys. B **16**, L443 (1983).

[13] Y. L. Luke, *Integrals of Bessel Functions* (McGraw-Hill, New York, 1962).

[14] *Handbook of Mathematical Functions,* Natl. Bur. Stand. Appl. Math. Ser. No. 55, edited by M. Abramowitz and I. A. Stegun (U.S. GPO, Washington, DC, 1965).

[15] I. S. Gradshteyn and I. M. Ryzhik, in *Tables of Integrals, Series and Products,* edited by A. Jeffrey (Academic, New York, 1980).